reverse correlation algorithm is used to identify the stimulus and hence to select a histogram bin to increment, except that the stimulus now consists of a pair of bars for the two eyes.

9. D. Ferster, *J. Physiol. (London)* **311**, 623 (1981).
10. Disparity tuning curves in all earlier studies have been obtained by sweeping a pair of bars with varying binocular disparities over the RFs. Such tuning curves may be predicted from our data by integrating the two-dimensional profiles of Fig. 3A along the constant disparity lines parallel to the 45° diagonal.
11. We cannot determine whether the elongated diagonal contours in Fig. 3A lie at zero disparity.
12. It is of interest to determine if there is a correlation between the preferred orientations of complex cells and the behavior of these neurons as disparity detectors. We have observed desired behavior for cells with a wide variety of preferred orientations. Our sample size is not currently sufficient to permit conclusions to be drawn in this regard.
13. Our model is a binocular generalization of a model proposed previously [D. A. Pollen and R. F. Ronner, *Vision Res.* **22**, 101 (1982); *IEEE Trans. Sys. Man Cybern.* **13**, 907 (1983); D. A. Pollen, J. P. Gaska, L. D. Jacobson, in *Models of Brain Function*, R. M. J. Cotterill, Ed. (Cambridge Univ. Press, Cambridge, 1989), p. 115].
14. D. Ferster, *J. Neurosci.* **8**, 1172 (1988); R. A. Stepnoski and L. A. Palmer, *Invest. Ophthalmol. Vis. Sci.* **30** (suppl.), 297 (1989); K. H. Foster *et al.*, *J. Physiol. (London)* **345**, 22P (1983).
15. Nearby simple cell pairs, recorded from a single electrode, show response phase differences of 90°, suggesting a quadrature relation of the pairs [D. A. Pollen and S. F. Ronner, *Science* **212**, 1409 (1981)].
16. Combining squared outputs of quadrature subunits provides smooth profiles for complex cell RFs. Such schemes are called "energy models" and were first used to describe mechanisms of motion perception [E. H. Adelson and J. R. Bergen, *J. Opt. Soc. Am.* **A2**, 284 (1985); R. C. Emerson, M. J. Korenberg, M. C. Citron, in *Advanced Methods of Physiological System Modeling*, V. Z. Marmarelis, Ed. (Plenum, New York, 1989), vol. 2, p. 97]. Our model, therefore, is an energy model of disparity detection.
17. A Gabor function is the product of a Gaussian and a sinusoid [D. Gabor, *J. Inst. Electr. Eng.* **93**, 429 (1946)]. The use of one-dimensional Gabor functions as RF profiles (Fig. 3B, insets) is consistent with two-dimensional models of simple-cell RFs proposed previously [J. Marcelja, *J. Opt. Soc. Am.* **70**, 1297 (1980); J. G. Daugman, *ibid.* **A2**, 1160 (1985); J. P. Jones and L. A. Palmer, *J. Neurophysiol.* **58**, 1233 (1987)]. This is because the one-dimensional RF as measured by a thin, long bar stimulus of optimal orientation, is given by the integral of the two-dimensional Gabor profile along the length of RF flanks. This integral, as shown below, is also a Gabor function with the same extent and spatial frequency as the two-dimensional function.

$$\int_{-\infty}^{\infty} G(x, y)dy = \int_{-\infty}^{\infty} \exp(-\alpha x^2 - \beta y^2)$$
$$\cos(2\pi fx + \theta)dy = A \exp(-\alpha x^2)\cos(2\pi fx + \theta)$$

where α and β are constants, f is the frequency, θ is the phase, and A is an integration constant. It is not necessary for the model to have even an odd symmetry for the RFs of quadrature pairs. Therefore, the model does not conflict with a previous finding that simple RF profiles are not generally even or odd symmetric [D. J. Field and D. J. Tolhurst, *Proc. R. Soc. London Ser. B* **228**, 379 (1986)].
18. G. F. Poggio and B. Fischer, *J. Neurophysiol.* **40**, 1392 (1977).
19. In the classification scheme of Poggio and Fischer (*18*), all categories are defined with respect to absolute disparity, whereas our system is defined in terms of phase at each spatial frequency scale. This difference is probably the reason why the former scheme needed the addition of two new categories (tuned-near, tuned-far) to the original four [G. F. Poggio *et al.*, *J. Neurosci.* **8**, 4531 (1988)].

20. Supported by NIH grant EY01175. We thank G. Ghose for help with the experiments and detailed review of the manuscript.

14 February 1990; accepted 8 June 1990

Activation of Extrastriate and Frontal Cortical Areas by Visual Words and Word-Like Stimuli

STEVEN E. PETERSEN, PETER T. FOX,* ABRAHAM Z. SNYDER, MARCUS E. RAICHLE

Visual presentation of words activates extrastriate regions of the occipital lobes of the brain. When analyzed by positron emission tomography (PET), certain areas in the left, medial extrastriate visual cortex were activated by visually presented pseudowords that obey English spelling rules, as well as by actual words. These areas were not activated by nonsense strings of letters or letter-like forms. Thus visual word form computations are based on learned distinctions between words and nonwords. In addition, during passive presentation of words, but not pseudowords, activation occurred in a left frontal area that is related to semantic processing. These findings support distinctions made in cognitive psychology and computational modeling between high-level visual and semantic computations on single words and describe the anatomy that may underlie these distinctions.

STUDIES IN COGNITIVE PSYCHOLOGY (*1–3*) and neurology (*4*) have supported the idea that there are complex computations made on words and word-like letter strings that link the visual input into a unit. For example, each letter of a word can be perceived at a lower threshold than when that letter is presented alone or as part of a nonsense string of letters (*3*). This perceptual advantage extends to pseudowords, meaningless letter strings that are similar to words (for example, POLT), but not to random strings of letters (for example, PXQLO) suggesting that this effect does not involve the meaning of the string but its regularity, that is, its similarity to strings of letters that would be words (*5*).

In an earlier study of single word processing, we showed that passively presented visual words activated a number of extrastriate areas bilaterally in the occipital lobes (*6*). In that study, only words were used as stimuli, thus there was no evidence that these activations were unique to words. Additionally, when subjects were required to generate the meaning of visual or auditory words, or to monitor a list of words for a semantic category, an area of the left prefrontal cortex was active, suggesting that this frontal region is related to semantic processing (*6*). In cognitive studies it has often been argued that some lexical and semantic processing is carried out automatically whenever a word is presented (*7*). This processing may involve areas within the left prefrontal cortex (*8*), but there was no evidence of activation of the left frontal area during passive presentation of words (*6*). To explore these issues further, we designed PET experiments to compare the areas activated during the visual representation of four different sets of word-like stimuli.

Subjects were normal volunteers between 18 and 49 years old. All subjects (n = 8, five males and three females) were native English speakers and strongly right-handed. Most subjects were students in the medical, allied health, or graduate schools of Washington University. These people, as a group, were assumed to be normal or above in reading skills and general intelligence.

The PET imaging, general task design, and data analysis strategies have been described and include (i) the use of ^{15}O-labeled water as a blood flow tracer [the short radioactive half-life (123 s) and scan time (40 s) of $[^{15}O]H_2O$ allow eight scans to be done in a single session (*9*)]; (ii) paired (task minus control) image subtraction to isolate areas of change between active and control conditions (*10*); (iii) intersubject image averaging to increase the signal strength of active regions compared to the noise background (*11*); (iv) a two-stage (omnibus and post hoc) statistical analysis to describe the significance of the foci in the averaged subtraction images (*11*).

Seven scans were performed on each subject. A fixation-point-only control scan was obtained while the subject fixated on a blank screen interposed between each of four stimulus-set scans (*12*). The order of presentation of stimulus sets was counterbalanced among individuals, and the order of presentation within sets was pseudorandomized.

S. E. Petersen, Department of Neurology and Neurological Surgery, Department of Anatomy and Neurobiology, Department of Psychology, and the McDonnell Center for Higher Brain Function, Washington University School of Medicine, 660 South Euclid, Box 8111, St. Louis, MO 63110.
P. T. Fox, A. Z. Snyder, M. E. Raichle, Department of Neurology and Neurological Surgery, Department of Radiology, Division of Radiation Science, Mallinckrodt Institute of Radiology, and the McDonnell Center for Higher Brain Function, Washington University School of Medicine, 660 South Euclid, Box 8111, St. Louis, MO 63110.

*Present address: The Johns Hopkins Hospital, Neuroradiology Section, Meyer 8-140, Baltimore, MD 21205.

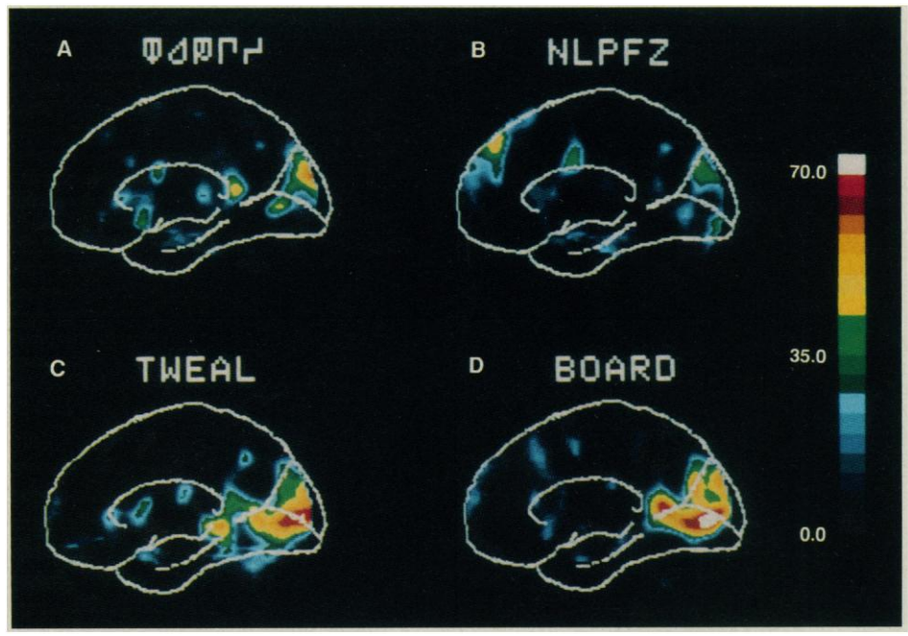

Fig. 1. PET images (single slices) taken from subtraction images averaged from all eight subjects show areas of increased blood flow (*9*) when presented with four different sets of word-like stimuli (compared to fixation point control). Each slice is taken from the same sagittal location 2 cm left of the midsagittal plane. The location of the slices is represented by the vertical dashed line in Fig. 3B. Anterior is at the left of each image. At the top of each section is a sample from the stimulus set that produced this activation. For both the false-font (**A**) and letter string (**B**) stimulus presentation there is little activation in the inferior and posterior part of the image. Pronounceable nonword (**C**) and real word stimulus presentation (**D**) produce clear activation, which consists of three identifiable foci (*15*).

There were four different sets of stimuli. During a single scan, members of only one set were presented. The four stimulus sets were (i) single common nouns (real words); (ii) nonwords that followed the spelling rules of English, that is, pseudoword strings like FLOOP and TOGLO (pseudowords); (iii) orthographically irregular groups of English characters like JVJFC (consonant letter strings); and (iv) strings of letter-like forms (false fonts) (*13*). These stimuli were designed to separate activations related to processing at the level of the simple visual properties of the stimuli, letters, orthographic and phonological regularity, or lexical-semantic processing where real words are discriminated from other letter strings on the basis of meaning.

All four stimulus sets produced lateral extrastriate responses. This activation indicates processing at a level common to all four stimulus sets, that is, the complex visual features of the stimuli. The foci of activation for each of these four conditions were identified by subtraction of a fixation scan from the test scan.

Real words and pseudowords produce responses in the left, medial extrastriate cortex (Fig. 1, C and D) (*14*) that are not seen with false fonts (Fig. 1A) or letter strings (Fig. 1B). Two explanations for the medial extrastriate activation by real and pseudowords were considered: (i) the activation is due to the fact that the string of letters follows the spelling rules of English and could be seen as a legitimate visual word form or (ii) the activation represents the difference between the pronounceability (phonological characteristics) of the pseudowords and real words on the one hand, and the false font and letter strings on the other. We believe that the visual word form argument seems stronger. The activation is posteriorly located near regions otherwise devoted to aspects of visual processing (*4*). These regions are activated by the visual presentation of words, but not by the auditory presentation of words (*6*). [An area in temporoparietal cortex that is commonly activated by auditory word presentation and by a task in which subjects had to make a phonological judgment on visually presented material have been described (*6*); howev-

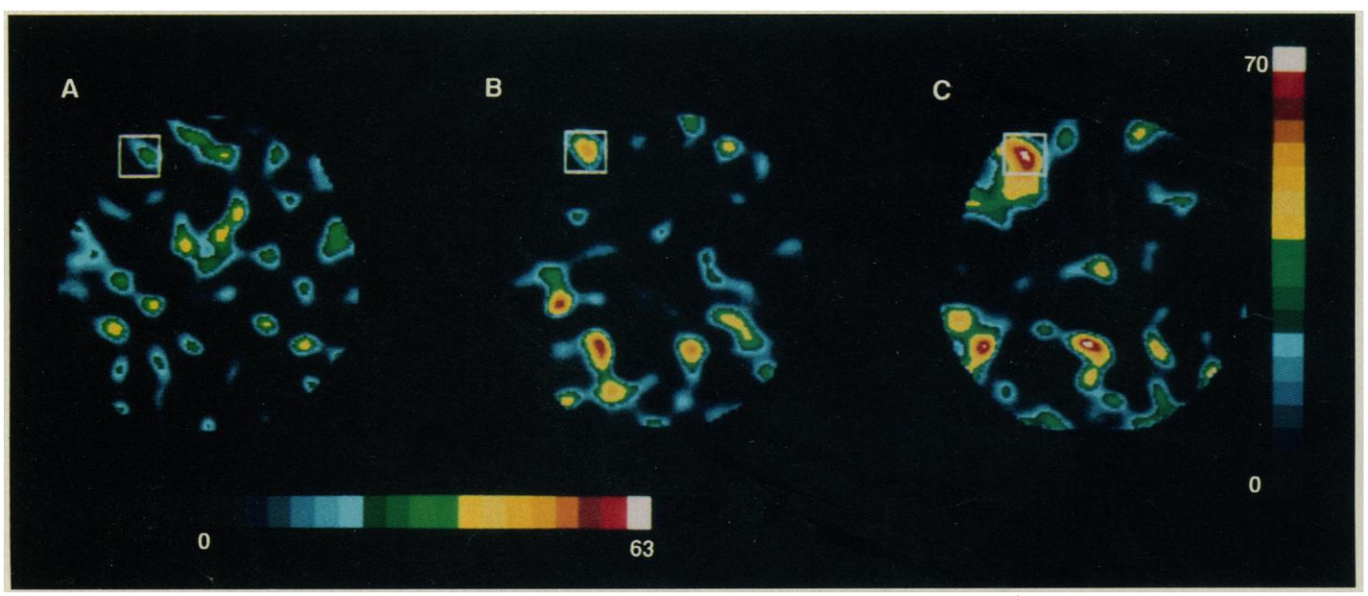

Fig. 2. PET images (single slices) taken from subtraction images averaged from all eight subjects show no increase in blood flow during presentation of pseudowords (**A**) but clear increased blood flow (*9*) in left prefrontal cortex (boxes) during the simple presentation of real words (**B**) and during an explicit semantic processing task (**C**) (*6*). The level of these slices is shown as the lower horizontal dashed line in Fig. 3B.

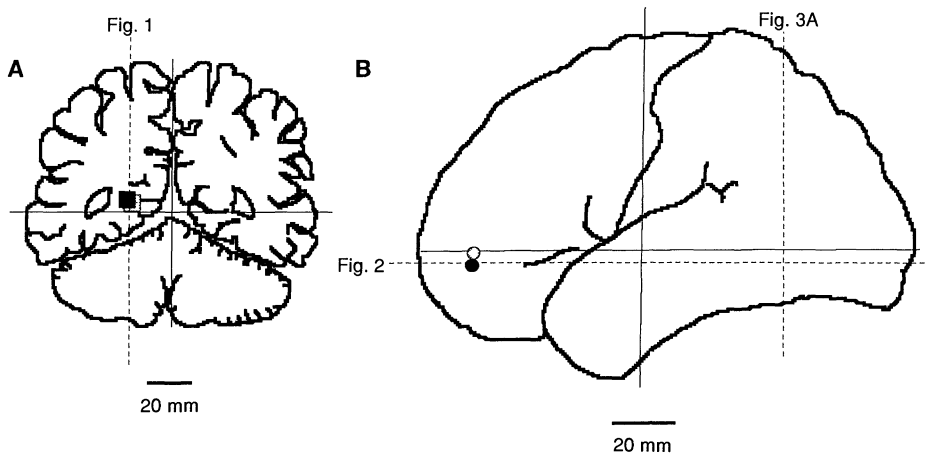

Fig. 3. (**A**) The medial extrastriate area activated by real words (filled square) and pronounceable nonwords (pseudowords) (shaded square). This area is not activated by presentation of letter strings and false font stimuli. The position of this slice is shown in (B); the position of the PET slices in Fig. 1 is shown. (**B**) A lateral view of the left hemisphere showing the inferior frontal areas activated by real words but not pseudowords. The orientation of the PET slice in Fig. 2 is shown. Visible presentation of real words produced activation at coordinates (z, x, y) = (0, +29, +55) (shaded circle), whereas the task in which people were asked to generate a semantic associate for a visually presented word produced activation at (−6, +28, +50) (filled circle).

er, this lateral temporoparietal "phonological" area is distant from the medial extrastriate areas we describe in this report.] Lesions in left occipitotemporal cortex often produce pure alexia, the inability to read without other language deficit (*4*).

Rules of spelling and orthography are specific to each language. The presence of a left-lateralized area in posterior, extrastriate cortex that distinguishes between letter strings that do and do not conform to English spelling rules argues that access to information specific to English orthography is present very early in the visual processing stream. These areas may represent the neural mechanism underlying the perceptual advantage that words and pseudowords show over irregular letter strings. Furthermore, such an area may be the cortical site for priming of word perception occurring at a presemantic level (*15*).

The statistical methodology that is used (*9*) is conservative in nature and encourages utilizing more subtle subtraction pairs if the possibility exists. For example, the false font conditions can act as the control condition for the other three stimulus sets, in essence subtracting away areas related to simple visual feature processing, isolating areas related to processes not shared in all conditions. As would be expected, activation is seen in left medial extrastriate cortex for both the real word and pseudoword subtractions. However, there is also a significant difference between these new images for real words and pseudowords. There is significant activation in the left frontal cortex in the real word, but not the pseudoword condition (Fig. 2, A and B). This locus is very close to that activated by semantic processing tasks in our earlier studies (Fig. 2C) (*6*).

The activation of a region of left frontal cortex by passive viewing of real words, but not pseudowords, and also by explicit semantic processing tasks (*6*) argues that this area is generally involved in some semantic computation on single words. Left frontal activation by passive presentation of visual words is the first indication from a PET study that this frontal region could be taking part in more automatic semantic priming tasks that are preferentially affected by frontal lesions (*8*) and that are separable from earlier types of processes, such as presemantic perceptual priming (*15, 16*).

Our results indicate that separate brain regions are activated by the presentation of stimulus sets that can be processed in different ways (at the visual feature level, orthographically, and semantically). These observations are consistent with distinctions from performance studies (*1*) that isolate these different processes, and aid in our understanding of the specific functional anatomy underlying them.

REFERENCES AND NOTES

1. M. I. Posner, *Chronometric Explorations of Mind* (Oxford Univ. Press, New York, 1986); D. LaBerge and J. Samuels, *Cogn. Psychol.* **6**, 293 (1974).
2. J. L. McClelland and D. E. Rumelhart, *Psychol. Rev.* **88**, 375 (1981).
3. G. M. Reicher, *J. Exp. Psychol.* **81**, 274 (1969).
4. A. R. Damasio and H. Damasio, *Neurology* **33**, 1573 (1983).
5. For a review see T. H. Carr and A. Pollatsek, in *Reading Research: Advances in Theory and Practice, Volume 5* [D. Besner, T. G. Waller, G. E. MacKinnon, Eds. (Academic Press, New York, 1985), pp. 1–82].
6. S. E. Petersen, P. T. Fox, M. I. Posner, M. A. Mintun, M. E. Raichle, *Nature* **331**, 585 (1988); *J. Cogn. Neurosci.* **1**, 153 (1989). For a review of other PET studies, see J. C. Mazziota and E. J. Metter, *Language, Communication, and the Brain* [F. Plum, Ed. (Raven, New York, 1988), pp. 245–266].
7. M. I. Posner and C. R. Snyder, *Attention and Performance V*, P. M. Rabbit, Ed. (Academic Press, New York, 1975); A. J. Marcel, *Cogn. Psychol.* **15**, 197 (1983).
8. W. Milberg, S. E. Blumstein, B. Dworetzky, *Brain Lang.* **31**, 138 (1987); G. Sartori, J. Masterson, R. Job, *The Cognitive Neuropsychology of Language*, M. Coltheart, G. Sartori, R. Job, Eds. (Erlbaum, Hillsdale, NJ, 1987), pp. 59–77; D. Swinney, E. Zurif, J. Nicol. *J. Cogn. Neurosci.* **1**, 25 (1989).
9. M. E. Raichle, W. R. W. Martin, P. Herscovitch, M. Mintun, J. Markham, *J. Nucl. Med.* **24**, 790 (1983). Because of the linear relation between blood flow (BF) and radioactivity in the tissue as measured by PET [P. Herscovitch, J. Markham, M. E. Raichle, *ibid.*, p. 782; P. T. Fox, M. A. Mintun, P. Herscovitch, M. E. Raichle, *J. Cereb. Blood Flow Metab.* **4**, 329 (1984)], we chose to forego measurement of arterial blood radioactivity in these studies and report our results simply as radioactive counts. Subjects' heads are immobilized within a closely fitted, thermally molded, plastic facial mask. A venous catheter is placed in one arm. Water labeled with ^{15}O acting as a BF tracer is administered as an intravenous bolus of 8 to 10 ml of saline containing 50 to 70 mCi. A 40-s scan is initiated when the bolus enters the brain. The PETT VI system is used in the low-resolution mode, simultaneously acquiring seven parallel slices with a center-to-center distance of 14.4 mm. Images are reconstructed by filtered backprojection to a resolution of 18 mm at full width at half maximum. The reconstructed images are of regional distribution of radiation. Images of change are obtained from each subject for each experimental condition by subtracting one image from another. These images are created after linear normalization that negates the effects of global BF fluctuations, both inter- and intrasubject. Through the use of a set of anatomical standardization techniques [P. T. Fox, J. S. Perlmutter, M. E. Raichle, *J. Comput. Assist. Tomogr.* **9**, 141 (1985)], single subtraction images are converted into anatomically standardized images and averaged across subjects to suppress image noise and improve signal-to-noise. The averaged subtraction images are then searched by an automatic maximum-detection algorithm to identify and record by magnitude and location (x, y, z stereotactic coordinates) all positive and negative local maxima. The distribution of BF change magnitudes obtained represents the signal plus noise distribution of an image. Most local maxima and minima in a subtraction image are noise and are randomly distributed. Image averaging suppresses noise while it fails to suppress the spatially nonrandom physiological responses. Physiological responses in averaged images will then be of greater magnitude than noise and are identified on that basis. The statistical analysis is two-tiered. First, an omnibus test (gamma-two statistic) is used to determine whether an image has any significant responses (distribution outliers). Second, as a post hoc analysis, the magnitude of a response is described relative to the noise level by Z score (response magnitude/distribution standard deviation); [(*11*); P. T. Fox and M. A. Mintun, *J. Nucl. Med.* **30**, 141 (1989)].
10. P. T. Fox *et al.*, *Nature* **323**, 806 (1986); P. T. Fox, F. M. Miezin, J. M. Allman, D. C. Van Essen, M. E. Raichle, *J. Neurosci.* 7, 913 (1987).
11. M. A. Mintun, P. T. Fox, M. E. Raichle, *J. Cereb. Blood Flow Metab.* **9**, 96 (1989); P. T. Fox, M. A. Mintun, E. M. Reiman, M. E. Raichle, *ibid.* **8**, 642 (1988).
12. During all scans, subjects were instructed to fixate on a small cross hair presented on a cathode ray tube display system suspended about 12 inches from the subject's head.
13. All four stimulus sets were equated for distribution of string lengths, which varied between 3 and 10 characters (mean, 5.5; mode, 5). The real word list was comprised of 256 animals and familiar household items (for example, FISH and CONTAINER).

The pseudowords were matched to the real words in probability of occurrence of each individual letter. The letter strings consisted of consonants. The false-font characters were composed of contiguous curved and straight-line segments designed to be at once dissimilar from any of the alphabetical symbols, but equivalent in the content of primitive visual features. Each character was generated on a 7 by 5 pixel grid. All four stimulus sets were matched in average number of pixels illuminated; vertical, horizontal, and oblique contours; and approximately matched in curvature, corners, and line segment intersections. These stimuli were presented once per second with an on-time of 150 ms.

14. The area of left, medial temporal cortex activated by visually presented words and pseudowords was composed of several identifiable foci of blood flow change. The stereotactic atlas coordinates of these foci were based on our system of anatomical localization with PET. The coordinates (z, x, y) were for real words: (+2, +29, −53), (+2, +21, −63), and (+6, +21, −41) for pseudowords: (+4, +23, −65) and (−47, +4, +19).
15. For a recent review of priming and human memory systems see E. Tulving and D. L. Schacter, *Science* **247**, 301 (1990).
16. M. I. Posner, J. Sandson, M. Dhawan, G. L. Shulman, *J. Cogn. Neurosci.* **1**, 50 (1989).
17. Supported by NIH (NS 06833, NS 25233, HL 13851) and the McDonnell Center for Studies of Higher Brain Function of Washington University. We thank M. Posner for his comments and H. Messmer for manuscript preparation.

8 February 1990; accepted 18 June 1990

Electrostatic and Steric Contributions to Regulation at the Active Site of Isocitrate Dehydrogenase

ANTONY M. DEAN AND DANIEL E. KOSHLAND, JR.

The isocitrate dehydrogenase of *Escherichia coli* is regulated by covalent modification at the active site rather than, as expected, at an allosteric site. As a means of evaluating the mechanism of regulation, the kinetics of the substrate, 2*R*,3*S*-isocitrate, and a substrate analog, 2*R*-malate, were compared for the native, phosphorylated, and mutant enzymes. Phosphorylation decreases activity by more than a factor of 10^6 for the true substrate, but causes minor changes in the activity of the substrate analog. The kinetic results indicate that electrostatic repulsion and steric hindrance between the phosphoryl moiety and the γ carboxyl group of 2*R*,3*S*-isocitrate are the major causes of the inactivation, with a lesser contribution from the loss of a hydrogen bond.

COVALENT REGULATION, PARTICULARLY by phosphorylation, is ubiquitous in biological systems (*1*). The discovery of covalent modification at the active site (*2*) raises questions concerning the mechanism of regulation. Phosphorylation of a Ser^{113} completely inactivates the isocitrate dehydrogenase (IDH) of *Escherichia coli* (*3–5*) by preventing isocitrate binding (*6*) and without significant conformational changes (*7*). Substitution for Ser^{113} by aspartate and glutamate also inactivates IDH, whereas substitutions by other amino acids do not (*5, 6*). It was postulated that electrostatic factors may play a dominant role in inactivation (*5*), and calculations suggest that such a repulsion could explain the findings (*2*).

Given the uncertainties in the electrostatic calculations on complex surfaces (*8*), independent corroborative evidence is required for assessing the relative contributions of various factors. To do this, the kinetic properties of a substrate, 2*R*,3*S*-isocitrate, and a substrate analog, 2*R*-malate, were compared with the use of native, phosphorylated, and mutant enzymes. Since catalysis occurs at the α and β carboxyl groups of 2*R*,3*S*-isocitrate, a compound (2*R*-malate) retaining the reactive groups of 2*R*,3*S*-isocitrate, but lacking the γ carboxyl that interacts with the phosphoryl moiety, might bind and serve as a substrate for the phosphorylated enzyme (Fig. 1).

Indeed 2*R*-malate, which has the same chirality as 2*R*,3*S*-isocitrate, is a substrate for IDH, whereas 2*S*-malate is not. As expected, the Michaelis constant (K_m) of the substrate analog is larger, and the maximum velocity is smaller than for the natural substrate isocitrate (Table 1). However, 2*R*-malate is also a substrate for the phosphorylated enzyme, whereas 2*R*,3*S*-isocitrate is not. In fact, phosphorylation has little effect on the Michaelis constant for 2*R*-malate (Table 1). Whereas substitutions with different amino acids for Ser^{113} have dramatic effects on the kinetic constants for 2*R*,3*S*-isocitrate, the effects on the kinetic constants for 2*R*-malate are much smaller. Thus, direct interactions between the γ carboxyl group of isocitrate and the side chain of residue 113 are primarily responsible for the regulation of IDH activity (Fig. 1).

The effects of phosphorylation can now be addressed quantitatively. Approximately, twofold changes in the isocitrate Michaelis constant and maximum activity can be attributed to the loss of the hydrogen bond with the γ carboxyl group of isocitrate as determined by the replacement of Ser^{113} with alanine ($V_{max}/V_{max\text{-}Ser} = 0.08$; $K_{m\text{-}Ala}/K_{m\text{-}Ser} = 1.8$ (*5*). The crystallographic structures show that overlaps between the Van der Waals radii of the side chains of glutamate, aspartate, phosphoserine, tyrosine, and lysine at site 113, and the γ carboxyl group of isocitrate are possible (*2*). The tyrosine and lysine residues, which have large overlaps, cause decreases in V/K_m by factors of 8.5×10^3 and 3.5×10^3, respectively (Table 1). The positively charged amino group of lysine may have an activating effect, but this is probably small because the amino group is so far removed from the γ

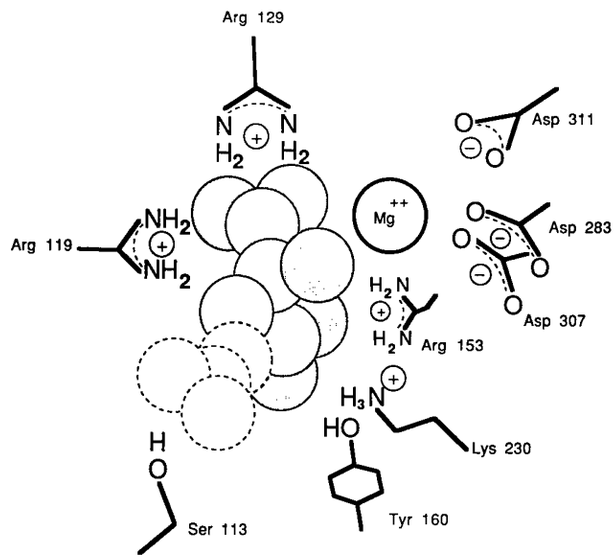

Fig. 1. 2*R*-malate (shaded spheres) and 2*R*,3*S*-isocitrate (shaded and dashed spheres) in the active site of IDH. The γ carboxyl group of 2*R*,3*S*-isocitrate (dashed spheres) hydrogen bonds to Ser^{113}, which is also the site of phosphorylation. The α, β, and γ carboxyl groups of 2*R*,3*S*-isocitrate hydrogen bond to three Arg^{119}, Arg^{129}, and Arg^{153}. The α carboxyl group and α hydroxyl group are chelated to a magnesium ion associated with Asp^{283} and Asp^{307} and the β carboxyl group hydrogen bonds to Tyr^{160} and Lys^{230}. During catalysis, the loss of a proton from the α hydroxyl group and the transfer of the hydrogen from the α carbon to nicotinamide adenine dinucleotide phosphate (NADP) results in dehydrogenation. The loss of the β carboxyl group as CO_2 is followed by protonation of the β carbon to form α-ketoglutarate.

Department of Molecular and Cell Biology, University of California, Berkeley, CA 94720.